Fluid Flow through Converging-Diverging Rocket Nozzles

Diya Mehta (22110078)

Department of Mechanical Engineering, IIT Gandhinagar

Under Prof. Dilip Srinivas Sundaram for the course ME 605: Computational Fluid Dynamics

1. Problem Statement

The purpose of this project is to perform a computational analysis of compressible, quasi-one-dimensional flow through a converging-diverging rocket nozzle.

The project aims to numerically simulate the flow through the nozzle under two different flow regimes:

1. Isentropic subsonic flow: In this regime, the flow remains subsonic throughout the nozzle.
2. Isentropic subsonic-supersonic flow: In this case, the flow accelerates to Mach 1 at the throat and becomes supersonic in the diverging section of the nozzle.

To ensure the accuracy of the simulation, the Euler equations governing the conservation of mass, momentum, and energy for compressible flow are solved in their conservative form. The MacCormack scheme, an explicit predictor-corrector method, is employed to numerically discretize the governing equations, ensuring second-order accuracy in both time and space. The simulation aims to reach a steady-state solution for each flow regime by time-marching the equations.

The flow behavior in the nozzle is heavily influenced by the back pressure applied at the outlet. By controlling the back pressure, different flow regimes can be established, allowing for the detailed analysis of subsonic, supersonic, and shock wave phenomena.

2. Mesh Details and Approach for Discretization

The accurate simulation of fluid flow through a converging-diverging rocket nozzle necessitates a meticulously constructed computational mesh and a discretization approach. This section outlines the mesh generation strategy and the discretization methodology employed to solve the governing Euler equations using the Finite Difference Method (FDM) with MacCormack's scheme.

2.1. Computational Domain and Geometry

The nozzle geometry is defined by the area function:

$$A(x) = 1 + 2.2(x - 1.5)^2 \quad \text{for } 0 \leq x \leq 3 \tag{1}$$

This represents a converging-diverging nozzle with the throat located at $x = 1.5$. The computational domain spans from $x = 0$ (inlet) to $x = 3$ (outlet), capturing the entire nozzle length.

2.2. Mesh Generation

2.2.1. Grid Type. A structured, one-dimensional (1D) grid is utilized, aligning with the quasi one-dimensional assumption of the flow. This simplifies the mesh generation process and aligns with the assumption that flow properties are uniform across any cross-sectional area of the nozzle.

2.2.2. Grid Resolution. **Number of Grid Points (n):** The computational domain is discretized into n equally spaced grid points. The choice of n balances computational efficiency with the need for sufficient resolution to capture flow features accurately. The grid of $n = 100$ points is chosen.

Grid Spacing (Δx): Given the nozzle length $L = 3$ units, the uniform grid spacing is:

$$\Delta x = \frac{L}{N-1} \tag{2}$$

2.3. Discretization Approach

The governing Euler equations are discretized using the Finite Difference Method (FDM), specifically employing MacCormack's explicit predictor-corrector scheme to achieve second-order accuracy in both space and time.

2.3.1. Spatial Discretization. **Grid Points Indexing:** Let i denote the spatial index, where $i = 1$ corresponds to $x = 0$ (inlet) and $i = N$ corresponds to $x = 3$ (outlet).

The governing equation for this system is:

$$\frac{\partial u}{\partial t} + \frac{\partial f}{\partial x} = 0$$

The MacCormack scheme for updating u at each time step can be expressed as:

$$u_i^{n+1} = u_i^n + \frac{\partial \bar{u}}{\partial t}\Delta t$$

where

$$\frac{\partial \bar{u}}{\partial t} = \frac{1}{2}\left(\frac{\partial u}{\partial t}\bigg|^n + \frac{\partial u}{\partial t}\bigg|^{n+1}\right)$$

In the predictor step, the time derivative at the n-th time level is approximated as (forward-differencing):

$$\frac{\partial u}{\partial t}\bigg|^n = -\frac{\partial f}{\partial x} \approx -\frac{f_{i+1}^n - f_i^n}{\Delta x}$$

The predicted value u_i^* at the intermediate step is:

$$u_i^* = u_i^n - \frac{\Delta t}{\Delta x}\left(f_{i+1}^n - f_i^n\right)$$

Using this prediction, the time derivative at $n+1$ is (backward-differencing):

$$\frac{\partial u}{\partial t}\bigg|^{n+1} = -\frac{\partial f}{\partial x} \approx -\frac{f_i^* - f_{i-1}^*}{\Delta x}$$

f^* is obtained using the predicted value of u^*. Substituting all these terms completes the MacCormack scheme.

2.3.2. Time Discretization. **Explicit Scheme:** MacCormack's method is an explicit scheme, requiring the time step Δt to satisfy the Courant–Friedrichs–Lewy (CFL) condition for numerical stability.

$$\Delta t \leq CFL \times \frac{\Delta x}{\max(|V| + C)} \tag{3}$$

where $C = \sqrt{\gamma RT}$ is the local speed of sound, and the maximum wave speed $|V| + C$ is evaluated across the entire domain. A CFL number CFL of 0.3 is chosen to ensure stability.

2.3.3. Boundary Conditions Implementation. Boundary conditions are implemented in terms of conserved variables.

- **Inlet ($i = 1$):** Reservoir conditions are imposed by setting $\rho_0 = \rho_{\text{stagnation}}$, V_0 is calculated from mass conservation, and energy (i.e temperature) is set based on stagnation conditions.
- **Outlet ($i = N$):** Depending on the flow regime, appropriate pressure conditions are enforced. Auxiliary conditions are applied using extrapolation based on characteristic analysis.

Numerical Stability: MacCormack's scheme inherently handles hyperbolic systems like the Euler equations. The explicit nature requires careful time step selection based on the CFL condition to maintain stability.

2.3.4. Discretization Steps.

1. **Initialization:** Set initial conditions for u based on intelligent guesses (e.g., linear profiles) for convergence.
2. **Time Marching:**
   - Predictor Step: Compute u_i^* using forward differencing.
   - Intermediate Flux Calculation: Evaluate f_i^* and based on u_i^*.
   - Corrector Step: Update u_i^{n+1} using backward differencing and average with predictor step.
   - Boundary Conditions: Apply inlet and outlet boundary conditions at each time step.
3. **Convergence Check:** Monitor residuals or changes in u to determine when steady-state is achieved.
4. **Iterate:** Repeat the time marching until convergence criteria are met.

3. Derivation and presentation of the final form of the discretized equations

This section presents the derivation of the discretized equations for quasi-one-dimensional, unsteady, compressible flow through a converging-diverging nozzle. The equations are expressed in conservation form, incorporating conserved variables, fluxes, and source terms. We employ the Finite Difference Method (FDM) and the MacCormack scheme to ensure second-order accuracy in both time and space.

3.1. Conservation Form of Governing Equations

The mass, momentum, and energy conservation equations for quasi-one-dimensional flow in conservative form are given below:

Continuity Equation

$$\frac{\partial(\rho A)}{\partial t} + \frac{\partial(\rho AV)}{\partial x} = 0 \tag{4}$$

where ρ is the density, A is the cross-sectional area, and V is the velocity.

Momentum Equation

$$\frac{\partial(\rho AV)}{\partial t} + \frac{\partial(\rho AV^2)}{\partial x} = -A\frac{\partial P}{\partial x} \tag{5}$$

where P is the pressure.

Total Energy Equation

$$\frac{\partial}{\partial t}\left(\rho A\left(e + \frac{V^2}{2}\right)\right) + \frac{\partial}{\partial x}\left(\rho AV\left(e + \frac{V^2}{2}\right)\right) = -\frac{\partial(PAV)}{\partial x} \tag{6}$$

where e is the internal energy.

3.2. Conservation Form of Governing Equations (Non-dimensionalized)

The non-dimensionalized continuity, momentum, and energy equations are given as follows:

Non-dimensionalized Continuity Equation

$$\frac{d(\rho' A')}{dt'} + \frac{d(\rho' A' V')}{dx'} = 0 \tag{7}$$

Non-dimensionalized Momentum Equation

$$\frac{d(\rho' A' V')}{dt'} + \frac{d\left(\rho' A' V'^2 + \frac{1}{\gamma}P' A'\right)}{dx'} = \frac{1}{\gamma}P'\frac{dA'}{dx'} \tag{8}$$

Non-dimensionalized Energy Equation

$$\frac{d\left(\rho'\left(\frac{e'}{\gamma-1} + \frac{\gamma}{2}V'^2\right)A'\right)}{dt'} + \frac{d\left(\rho'\left(\frac{e'}{\gamma-1} + \frac{\gamma}{2}V'^2\right)V'A' + P'A'V'\right)}{dx'} = 0 \tag{9}$$

The general conservation equations for quasi-one-dimensional flow are expressed as:

$$\frac{\partial Q}{\partial t'} + \frac{\partial F}{\partial x'} = S \tag{10}$$

Where:

- Q is the vector of conserved variables,
- F is the flux vector,
- S is the source term vector.

These equations correspond to the Euler equations for compressible flow, encompassing the conservation of mass, momentum, and energy.

3.2.1. Conserved Variables (Q). The vector Q contains the conserved quantities:

$$Q = \begin{bmatrix} \rho' A' \\ \rho' A' V' \\ \rho' A' \left(e' + \frac{V'^2}{2}\right) \end{bmatrix} \tag{11}$$

3.2.2. Flux Vector (F). The flux vector F represents the transport of conserved quantities through the control volumes:

$$F = \begin{bmatrix} \rho' A' V' \\ \rho' A' V'^2 + \frac{1}{\gamma} P' A' \\ \rho A' V' \left(\frac{e'}{\gamma-1} + \frac{\gamma}{2} V'^2\right) + P' A' V' \end{bmatrix} \tag{12}$$

3.2.3. Source Term Vector (S). The source term S accounts for the effects of the varying cross-sectional area of the nozzle:

$$S = \begin{bmatrix} 0 \\ \frac{1}{\gamma} P' \frac{\partial A'}{\partial x'} \\ 0 \end{bmatrix} \tag{13}$$

Here, Q_1, Q_2, Q_3 are the solution vectors. Using them, we find the primitive variables (ρ', V', T', P').

$$\rho' = \frac{Q_1}{A'} \tag{14}$$

$$V' = \frac{Q_2}{Q_1} \tag{15}$$

$$T' = e' = (\gamma - 1)\left(\frac{Q_3}{Q_1} - \frac{\gamma}{2} V'^2\right) \tag{16}$$

$$P' = \rho' T' \tag{17}$$

Using Q_1, Q_2, Q_3, we also find the flux terms (F_1, F_2, F_3) and source term (S_2).

$$F_1 = Q_1 \tag{18}$$

$$F_2 = \frac{Q_2^2}{Q_1} + \frac{\gamma - 1}{\gamma}\left(Q_3 - \frac{\gamma}{2}\frac{Q_2^2}{Q_1}\right) \tag{19}$$

$$F_3 = \frac{\gamma Q_2 Q_3}{Q_1} - \frac{\gamma(\gamma - 1)}{2}\frac{Q_2^3}{Q_1^2} \tag{20}$$

$$S_2 = \frac{1}{\gamma}\frac{Q_1}{A'}(\gamma - 1)\left[\frac{Q_3}{Q_1} - \frac{\gamma}{2}\left(\frac{Q_2}{Q_1}\right)^2\right]\frac{\partial A'}{\partial x'} \tag{21}$$

3.3. Discretization Using the MacCormack Scheme

To solve the conservation equations numerically, we discretize them using the MacCormack scheme, which consists of a predictor and a corrector step. The spatial domain is divided into grid points, and the temporal domain is divided into time steps.

3.3.1. Predictor Step (Forward Difference in Space). In the predictor step, we calculate the predicted values Q_i^* using forward differences:

$$\left.\frac{\partial Q}{\partial t'}\right|^n = -\frac{\partial F}{\partial x'} \approx -\frac{F_{i+1}^n - F_i^n}{\Delta x'} + S_i^n$$

$$Q_i^* = Q_i^n - \frac{\Delta t'}{\Delta x'}\left(F_{i+1}^n - F_i^n\right) + \Delta t' \cdot S_i^n \tag{22}$$

Where:

- Q_i^n: Conserved variables at the i-th grid point at time step n,
- F_i^n: Flux vector at the i-th grid point at time step n,
- S_i^n: Source term at the i-th grid point at time step n,
- Δt: Time step size,
- Δx: Spatial step size.

This step predicts the values of the conserved variables Q at an intermediate time $t^{n+\Delta t}$ i.e $Q_i^* = Q_i^{n+\Delta t}$.

At this step, using the predicted value of Q_i^* we find the predicted value of ρ' and T', and the flux terms, required for the corrector step.

3.3.2. Corrector Step (Backward Difference in Space). In the corrector step, we update the values of Q using backward differences:

$$\left.\frac{\partial Q}{\partial t'}\right|^{n+1} = -\frac{\partial F}{\partial x'} + S \approx -\frac{F_i^* - F_{i-1}^*}{\Delta x'} + S_i^*$$

$$Q_i^{n+1} = Q_i^n + \frac{\partial \bar{Q}}{\partial t'}\Delta t'$$

where

$$\frac{\partial \bar{Q}}{\partial t} = \frac{1}{2}\left(\left.\frac{\partial Q}{\partial t'}\right|^n + \left.\frac{\partial Q}{\partial t'}\right|^{n+1}\right)$$

Where:

- Q_i^*: Predicted values from the predictor step,
- F_i^*: Flux vector at the intermediate time step (from the predictor step),
- S_i^*: Source term at the intermediate time step.

This corrector step averages the predicted and initial values to obtain the updated conserved variables at the next time step t^{n+1}.

4. Solution Methodology

The solution methodology for simulating the compressible flow through a converging-diverging rocket nozzle involves discretizing the governing Euler equations in their conservative form and solving them numerically using the MacCormack scheme. The main goal is to compute the steady-state flow field for different flow regimes (subsonic and subsonic-supersonic cases) by time-marching the solution until convergence.

4.1. Problem Setup

The flow through the converging-diverging nozzle is governed by the Euler equations in conservative form, which represent the conservation of mass, momentum, and energy. These equations can be expressed as:

$$\frac{\partial Q}{\partial t'} + \frac{\partial F}{\partial x'} = S \tag{23}$$

Where:

- Q is the vector of conserved variables (mass, momentum, and energy),
- F is the flux vector (representing transport of these conserved quantities),
- S is the source term vector (accounting for area changes in the nozzle).

The nozzle's geometry is defined by the area function:

$$A(x) = 1 + 2.2(x - 1.5)^2 \quad \text{for } 0 \leq x \leq 3 \tag{24}$$

The flow properties vary only in the axial direction x, and the flow is assumed to be inviscid, adiabatic, compressible, and quasi-one-dimensional.

4.2. Discretization of Governing Equations

The Euler equations are discretized using the Finite Difference Method (FDM), applying the MacCormack scheme for time integration. The MacCormack method is an explicit, two-step predictor-corrector scheme that provides second-order accuracy in both time and space.

4.2.1. Predictor Step. A forward difference in space is used to predict the solution at an intermediate time.

4.2.2. Corrector Step. A backward difference in space is applied to correct the predicted solution and update the conserved variables. The discretized form of the conservation equations is:

$$Q_i^{n+1} = Q_i^n + \frac{\partial \bar{Q}}{\partial t'} \Delta t'$$

Where:

- Q: Conserved variables (mass, momentum, energy),
- Δt: Time step size,
- Δx: Grid spacing in the axial direction.

This time-marching approach is used to update the flow properties at each time step until a steady-state solution is achieved.

4.3. Boundary and Initial Conditions

To solve the Euler equations, boundary and initial conditions must be specified:

4.3.1. Inlet Boundary Conditions. Subsonic Inflow : At the subsonic inflow boundary, two properties are fixed, one is allowed to float. Thus, at i=1 we have:

$$\rho'_{(i=1)} = 1 \tag{25}$$
$$T'_{(i=1)} = 1 \tag{26}$$
$$Q_{1(i=1)} = (\rho' A')\,(i = 1) \tag{27}$$
$$Q_{2(i=1)} = 2Q_{2(i=2)} - Q_{2(i=3)} \tag{28}$$
$$V'_{(i=1)} = \frac{Q_{2(i=1)}}{Q_{1(i=1)}} \tag{29}$$
$$Q_{3(i=1)} = Q_{1(i=1)} \left(\frac{T'_{(i=1)}}{\gamma - 1} + \frac{\gamma}{2} V'^2_{(i=1)} \right) \tag{30}$$

The inlet is assumed to have known stagnation properties (stagnation pressure, stagnation density, and stagnation temperature). Velocity is initialized based on these stagnation conditions, ensuring non-zero velocity at the inlet.

4.3.2. Outlet Boundary Conditions. Different outlet pressures (back pressures) are specified depending on the flow regime being simulated:

- For subsonic flow, the outlet pressure is set close to the stagnation pressure.

$$P'_{(i=N)} = 0.99 \tag{31}$$
$$Q_{1(i=N)} = 2Q_{1(i=N-1)} - Q_{1(i=N-2)} \tag{32}$$
$$\rho'_{(i=N)} = \frac{Q_{1(i=N)}}{A'_{(i=N)}} \tag{33}$$
$$T'_{(i=N)} = \frac{P'_{(i=N)}}{\rho'_{(i=N)}} \tag{34}$$
$$Q_{2(i=N)} = 2Q_{2(i=N-1)} - Q_{2(i=N-2)} \tag{35}$$
$$V'_{(i=N)} = \frac{Q_{2(i=N)}}{Q_{1(i=N)}} \tag{36}$$
$$Q_{3(i=N)} = Q_{1(i=N)} \left(\frac{T'_{(i=N)}}{\gamma - 1} + \frac{\gamma}{2} V'^2_{(i=N)} \right) \tag{37}$$

- For supersonic flow, the flow properties at the outlet boundary are obtained by linear extrapolation from two adjacent internal points.

$$Q_{1(i=N)} = 2Q_{1(i=N-1)} - Q_{1(i=N-2)} \tag{38}$$
$$Q_{2(i=N)} = 2Q_{2(i=N-1)} - Q_{2(i=N-2)} \tag{39}$$
$$Q_{3(i=N)} = 2Q_{3(i=N-1)} - Q_{3(i=N-2)} \tag{40}$$

4.3.3. Initial Conditions. The initial guess for the flow properties is taken to be a linear distribution of variables based on knowledge of the flow regime (e.g., subsonic velocity).

- For subsonic flow,

To initialize the density ρ and temperature T profiles along a spatial domain x for each spatial index i, we define the conditions as follows:

For $i = 1, \dots, \text{nx}$:

- If $0 \leq x(i) < 0.5$:

$$\rho'(i) = 1, \quad T'(i) = 1$$

This represents the initial density and temperature.

- If $0.5 \leq x(i) < 1.5$:

$$\rho'(i) = 1 - 0.3 \cdot (x(i) - 0.5)$$

$$T'(i) = 1 - 0.2 \cdot (x(i) - 0.5)$$

This creates a linearly decreasing profile for both density and temperature until $x = 1.5$.

- If $x(i) \geq 1.5$:

$$\rho'(i) = 0.7 + 0.219 \cdot (x(i) - 1.5)$$

$$T'(i) = 0.8 + 0.107 \cdot (x(i) - 1.5)$$

This creates a linearly increasing profile for both density and temperature after $x = 1.5$.

- For supersonic flow,

For $i = 1, \dots, \text{nx}$:

- If $0 \leq x(i) < 0.5$:

$$\rho'(i) = 1, \quad T'(i) = 1$$

Initial density and temperature are set.

- If $0.5 \leq x(i) < 1.5$:

$$\rho'(i) = 1 - 0.3 \cdot (x(i) - 0.5)$$

$$T'(i) = 1 - 0.1 \cdot (x(i) - 0.5)$$

The density and temperature linearly decrease up to $x = 1.5$.

- If $1.5 \leq x(i) \leq 3$:

$$\rho'(i) = 0.7 - 0.3 \cdot (x(i) - 1.5)$$

$$T'(i) = 0.9 - 0.3 \cdot (x(i) - 1.5)$$

This section defines a linearly decreasing profile of density and temperature after $x = 1.5$.

4.4. Time Stepping and Stability Criteria

Since the MacCormack method is an explicit scheme, the Courant-Friedrichs-Lewy (CFL) condition must be satisfied to ensure numerical stability. The CFL condition dictates the size of the time step Δt and is calculated as:

$$CFL = \frac{(V_{\max} + \sqrt{T})\Delta t}{\Delta x} \tag{41}$$

For stability, the CFL number must be less than 1. Here, CFL=0.3 is chosen to ensure stability, and the time step is dynamically adjusted based on the local flow conditions.

4.5. Convergence to Steady-State

The simulation is marched forward in time until the solution reaches a steady-state condition or until the number of end of the time steps. This is determined when the change in conserved variables between time steps becomes sufficiently small, typically by monitoring the residuals of the governing equations:

$$\text{Residual} = \sum_i |Q_i^{n+1} - Q_i^n| \tag{42}$$

The simulation is stopped once the residuals fall below a specified tolerance (10^{-6}).

5. Results and discussion

In this section, the results obtained from the numerical simulation of compressible flow through the converging-diverging nozzle are presented and analyzed. Two different flow regimes were simulated: isentropic subsonic flow and isentropic subsonic-supersonic flow. The numerical results for each case are compared with analytical predictions where applicable, and the flow behavior is explained in terms of the physical phenomena occurring within the nozzle. Key flow properties such as pressure, density, temperature, and Mach number are plotted along the length of the nozzle, and the trends observed are discussed in detail.

5.1. Isentropic Subsonic-Supersonic Flow

5.1.1. Numerical Results. For the isentropic subsonic-supersonic flow case, the back pressure at the outlet was lowered significantly, causing the flow to reach supersonic conditions in the diverging section of the nozzle.

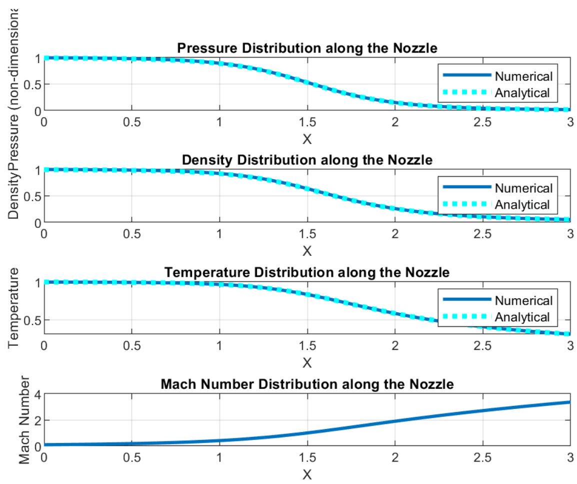

Figure 1. *Variation along the length*

- **Pressure:** The pressure decreases monotonically from the inlet to the outlet, with the most significant drop occurring in the diverging section.

- **Density:** The density follows a similar trend, decreasing sharply in the diverging section as the flow accelerates.

- **Temperature:** The temperature drops as the flow velocity increases, especially in the diverging section.

- **Mach Number:** The Mach number reaches 1 at the throat (sonic conditions) and continues to increase in the diverging section, achieving supersonic values at the nozzle exit.

5.1.2. Discussion. In this regime, the flow exhibits classical behavior for a converging-diverging nozzle. The flow accelerates to Mach 1 at the throat due to the choking phenomenon, where the mass flow rate is maximized. Beyond the throat, the flow enters the supersonic regime, with the velocity increasing rapidly and the pressure, density, and temperature decreasing correspondingly. This result matches the analytical predictions for isentropic flow in a converging-diverging nozzle.

5.2. Isentropic Subsonic Flow

5.2.1. Numerical Results. In the isentropic subsonic flow case, the back pressure at the outlet was set only slightly lower than the stagnation pressure, ensuring subsonic conditions throughout the nozzle. The flow accelerates in the converging section and decelerates in the diverging section.

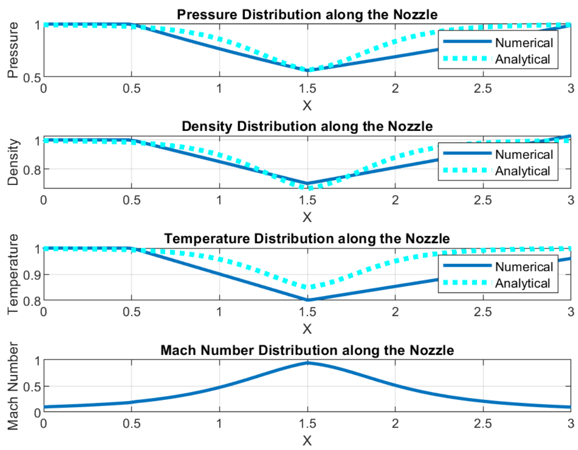

Figure 2. *Variation along the length*

- **Pressure:** The pressure decreases as the flow accelerates in the converging section, reaches a minimum at the throat, and then increases in the diverging section.
- **Density:** The density follows a similar trend to pressure, decreasing in the converging section and increasing in the diverging section.
- **Temperature:** The temperature decreases as the velocity increases in the converging section, then rises again in the diverging section due to the deceleration of the flow.
- **Mach Number:** The Mach number remains below 1 throughout the nozzle, peaking near the throat and then decreasing in the diverging section.

5.2.2. Discussion. The isentropic subsonic flow behaves similarly to an incompressible flow, as predicted by compressible flow theory. The conservation of mass in the converging section causes the velocity to increase, leading to a corresponding drop in pressure and density. As the flow decelerates in the diverging section, pressure and density increase. The Mach number never exceeds 1, confirming the subsonic nature of the flow. The numerical results do not perfectly align with the analytical isentropic flow solutions, but the solution gives a good approximation.

It was observed that the MacCormack method provided approximate solution only when certain parameters were carefully controlled. Specifically, the time step needed to be chosen in line with the Courant-Friedrichs-Lewy (CFL) condition to prevent instabilitiess. When the time step was too large, the solution exhibited oscillations and instability, whereas a smaller, CFL-compliant time step helped stabilize the results. Additionally, a finer grid resolution was essential for capturing smooth variations in purely subsonic flows, and the boundary conditions required careful setup.

The MacCormack method works well for flows that move from subsonic to supersonic speeds but has issues with purely subsonic cases. In subsonic flows, small disturbances can lead to unstable oscillations, as the method isn't ideal for handling sudden changes smoothly. Stability also depends on the Courant-Friedrichs-Lewy (CFL) condition, and since subsonic flows can have varying velocities, smaller time steps may be needed, which affects performance. Subsonic flows are also more sensitive to boundary conditions, which can worsen stability. In subsonic-supersonic flows, however, strong wave interactions make the MacCormack method more effective and stable.

5.3. Comparison with Analytical Solutions

For the isentropic flow regimes, the numerical results were compared with the analytical solutions derived from isentropic relations for compressible flow. The comparisons show excellent agreement for the isentropic subsonic-supersonic case and provides an approximate solution for the subsonic case. The accuracy of the MacCormack method in capturing the correct flow behavior is evident from the close match between the numerical and theoretical results.

5.4. Impact of Numerical Methodology

The MacCormack scheme used for discretization proved effective in resolving isentropicflows. The explicit time-stepping method, combined with second-order accuracy in both time and space, allowed for stable and accurate simulations. The use of the conservative form of the Euler equations ensured the conservation of mass, momentum, and energy throughout the domain.

However, it is important to note that the CFL condition imposed constraints on the time step size, with smaller time steps required to ensure stability.

6. Concluding Remarks

The Euler equations, which govern the conservation of mass, momentum, and energy, were solved in their conservative form using the Finite Difference Method (FDM) and the MacCormack scheme, ensuring second-order accuracy in both time and space.

6.0.1. Isentropic Subsonic Flow. The results demonstrated typical subsonic behavior (it followed the trend), with the flow accelerating in the converging section and decelerating in the diverging section. The pressure and density trends observed were consistent with compressible flow theory, and the numerical results aligned approximately with analytical solutions for isentropic flow.

6.0.2. Isentropic Subsonic-Supersonic Flow. The flow transitioned smoothly from subsonic to supersonic speeds, with the Mach number reaching 1 at the throat and increasing in the diverging section. The numerical method accurately captured the acceleration and expansion of the flow, with the results matching analytical predictions for isentropic supersonic flow in a converging-diverging nozzle.

6.0.3. Boundary Conditions. The accuracy of the results depended on the appropriate specification of boundary conditions, particularly at the outlet. Small changes in the back pressure had a significant impact on the flow regime.

7. Acknowledgements

I would like to express my sincere gratitude to Professor Dilip Srinivas Sundaram for his invaluable guidance and support throughout this project. I am also deeply thankful to the teaching assistants, Pardha Sai Mutyala and Malay Vyas, for their assistance and feedback.